Multielectron Oxidation of Anthracenes with a One-Electron Oxidant via Water-Accelerated Electron-Transfer Disproportionation of the Radical Cations as the Rate-Determining Step

Shunichi Fukuzumi,* Ikuo Nakanishi, and Keiko Tanaka

Department of Material and Life Science, Graduate School of Engineering, Osaka University, Suita, Osaka 565-0871, Japan

Received: February 15, 1999

The six-electron oxidation of anthracene and the four-electron oxidation of 9-alkylanthracene occur with $[Ru(bpy)_3]^{3+}$ (bpy = 2,2-bipyridine) in acetonitrile (MeCN) containing H_2O to yield anthraquinone and 10-alkyl-10-hydroxy-9(10H)anthracenone, respectively. The direct detection of radical cations of anthracene and its derivatives formed in the multielectron oxidation with $[Ru(bpy)_3]^{3+}$ and the extensive kinetic analysis are performed with the use of a stopped-flow technique. Both the rates of decay of anthracene radical cations and the formation of $[Ru(bpy)_3]^{2+}$ obey the second-order kinetics. The kinetic deuterium isotope effects and the dependence of the rates on the concentrations of $[Ru(bpy)_3]^{3+}$, anthracenes, and H_2O have revealed that the six-electron oxidation of anthracene and the four-electron oxidation of alkylanthracene proceed via the rate-determining electron-transfer disproportionation of radical cations of anthracene and alkylanthracene, which is accelerated by H_2O due to the complex formation between the corresponding dications and H_2O. The electron-transfer disproportionation of anthracene radical cations is followed by the facile nucleophilic attack of H_2O on the resulting dication leading to six-electron oxidized product, i.e., anthraquinone associated with rapid electron transfer from $[Ru(bpy)_3]^{3+}$ and anthracene radical cation in the presence of more than 6 equiv of $[Ru(bpy)_3]^{3+}$ and less than 1 equiv of $[Ru(bpy)_3]^{3+}$, respectively. The reorganization energy for the self-exchange between 9,10-dimethylanthracene and the radical cation in MeCN is also determined by analyzing line width variations of the ESR spectra at different concentrations of 9,10-dimethylanthracene. The reorganization energy is used to evaluate the rate constant of electron-transfer disproportionation of 9,10-dimethylanthracene radical cations in light of the Marcus theory of electron transfer, which agrees with the experimental value determined from the second-order decay of the radical cations.

Introduction

Electron-transfer oxidation of aromatic hydrocarbons has long attracted considerable interest in view of a drastic change in the reactivity of the radical cations which become much stronger acids, electrophiles, or oxidants than the parent molecules.[1−5] For example, the radical cation of toluene has a tremendous acidity ($pK_a = -13$)[4] and thereby the deprotonation from the alkylbenzene radical cations is the predominant decay process of the radical cations.[6−8] In the case of alkylanthracene radical cations which are much weaker acids (e.g., $pK_a = -6$ for 9,-10-dimethylanthracene radical cation)[4] as compared with toluene radical cation, the deprotonation leading to the side chain oxidation is known to be sluggish relative to nucleophilic attack by nucleophiles leading to the ring oxidation.[9−11] The low reactivity of nucleophiles toward radical cations has earlier been noted by Eberson.[12] These reactions are classified by Pross as "forbidden" because of the double excitation in the curve crossing diagram with respect to the ground state of the nucleophile/radical cation pair in contrast with "allowed" reactions of regular cations.[13] The "allowed−forbidden" classification was caught in a dilemma, since the rapid rates (10^7-10^9 M^{-1} s^{-1}) of radical cations of anthracene derivatives with strong base nucleophiles were reported and compared with the rates of regular cations.[14] Shaik and Pross then re-evaluated the "allowed−forbidden" classification based on a semiquantitative analysis to show that double excitation can often be small when the energy gap of both an electron transfer and a singlet−triplet excitation is small.[15] To gain more comprehensive and confirmative understanding of the reactions of radical cations with nucleophiles, it is certainly desired to obtain more kinetic data by detecting the transient radical cations directly to follow the reactions. In this regard, nanosecond laser flash photolysis or pulse radiolysis techniques have frequently been applied to obtain a time-resolved spectroscopic evaluation of the kinetics of the reactions of radical cations with nucleophiles.[16−21] However, there have so far been no kinetic studies of radical cation intermediates detected directly in multielectron oxidation of aromatic compounds such as the six-electron oxidation of anthracene to anthraquinone, although anodic six-electron oxidation of anthracene to anthraquinone has been long known.[22] The electrochemical method for the detection of radical cation intermediates is limited to studies involving stable radical cations such as the radical cation derived from 9,10-diphenylanthracene.[23]

This study reports the first direct detection of radical cations of anthracene and its derivatives formed in the multielectron oxidation with $[Ru(bpy)_3]^{3+}$ (bpy = 2,2′-bipyridine) in acetonitrile (MeCN) containing H_2O and the extensive kinetic analysis for the decay of the radical cations with use of a stopped-flow technique combined with the characterization of the oxygenated products.[24] The self-exchange rate constant between 9,10-dimethylanthracene and the radical cation in MeCN is also

10.1021/jp990541e CCC: $18.00
Published on Web 11/25/1999

determined by analyzing line width variations of the ESR spectra at different concentrations of 9,10-dimethylanthracene in order to estimate the rate of electron transfer between the radical cations. Simultaneous determination of the decay rates of anthracene radical cation and the rates of reduction of $[Ru(bpy)_3]^{3+}$ to $[Ru(bpy)_3]^{2+}$, the kinetic deuterium isotope effects and the dependence of the rates on the concentrations of $[Ru(bpy)_3]^{3+}$ and H_2O provide valuable and comprehensive insight into the mechanistic aspects in the multielectron oxidation.

Experimental Section

Materials. Anthracene and 9,10-dimethylanthracene were obtained from Tokyo Chemical Industry Co., Ltd., Japan and recrystallized from ethanol prior to use. Anthraquinone was purchased from Aldrich and recrystallized from chloroform. 9-Ethylanthracene and 9-benzylanthracene were prepared from Grignard reaction of anthrone with the corresponding alkylmagnesium bromide and purified through an alumina column. Tris(2,2′-bipyridine)ruthenium dichloride hexahydrate, $[Ru(bpy)_3]Cl_2 \cdot H_2O$, was obtained commercially from Aldrich. The oxidation of $[Ru(bpy)_3]Cl_2$ with lead dioxide in aqueous H_2SO_4 gives $[Ru(bpy)_3]^{3+}$ which was isolated as the PF_6 salt, $[Ru(bpy)_3](PF_6)_3$.[25] 1-Benzyl-1,4-dihydronicotinamide was prepared by the literature method.[26] Tris(1,10-phenanthroline)iron(III) perchlorate, $[Fe(phen)_3](ClO_4)_3$, was prepared by oxidizing the iron(II) complex with ceric sulfate in aqueous H_2SO_4.[27] Anhydrous magnesium perchlorate was obtained from Nakalai Tesque, Inc. Tetra-*n*-butylammonium perchlorate (TBAP) was purchased from Sigma Chemical Co., recrystallized from ethanol, and dried under vacuum at 40 °C prior to use. Acetonitrile was purchased from Wako Pure Chemical Ind. Ltd. and purified by successive distillation over CaH_2 according to standard procedures.[28]

Reaction Procedure. The isolation of the oxidation products was obtained by ether extraction. The isolated yield of anthraquinone was 91%. MS *m*/*z* 208 (M^+). ^1H NMR measurements were performed using a JNM-GSX-400 NMR spectrometer. ^1H NMR ($CDCl_3$) δ 7.86−7.89 (m, 4H), 8.25−8.28 (m, 4H). The isolated yield of 10-benzyl-10-hydroxy-9(10H)anthracenone was 80%. MS *m*/*z* 300 (M^+). ^1H NMR ($CDCl_3$) δ 2.61 (s, 1H), 3.22 (s, 2H), 6.13 (d, 2H, $J = 7.3$ Hz), 6.89 (t, 2H, $J = 7.5$ Hz), 7.04 (t, 1H, $J = 7.5$ Hz), 7.45 (t, 2H, $J = 7.8$ Hz), 7.66 (t, 2H, $J = 7.8$ Hz), 7.90 (d, 2H, $J = 7.8$ Hz), 8.03 (d, 2H, $J = 7.8$ Hz). 10-Ethyl-10-hydroxyanthrone: ^1H NMR (CD_3CN) δ 0.29 (t, 3H, $J = 7.3$ Hz), 1.98 (q, 2H, $J = 7.3$ Hz), 7.4−7.6 (m, 2H), 7.73 (t, 2H, $J = 7.3$ Hz), 7.92 (d, 2H, $J = 7.8$ Hz), 8.15 (d, 2H, $J = 7.8$ Hz).

Spectral and Kinetic Measurements. Typically, a 10 μL aliquot of $[Ru(bpy)_3](PF_6)_3$ (6.3×10^{-3} M) in MeCN containing H_2O (7.0×10^{-3} M) was added to a quartz cuvette (10 mm i.d.) which contained anthracene (2.1×10^{-5} M) in deaerated MeCN (3.0 mL). The concentration of H_2O in MeCN was determined by the complex formation of 1-benzyl-1,4-dihydronicotinamide with anhydrous magnesium perchlorate according to the literature method.[29] UV−visible spectral changes associated with the oxidation with different concentrations of $[Ru(bpy)_3](PF_6)_3$ were monitored using a Hewlett-Packard 8453 diode array spectrophotometer. The same procedure was used for spectral measurements for the oxidation of alkylanthracenes (RAn) with $[Ru(bpy)_3](PF_6)_3$. All measurements were carried out in a dark cell compartment using deaerated solutions to avoid the photochemical reactions of anthracenes.

Kinetic measurements of the oxidation of anthracene and 9-alkylanthracene with $[Ru(bpy)_3](PF_6)_3$ in MeCN containing various concentrations of H_2O were carried out using a Union RA-103 stopped-flow spectrophotometer under deaerated conditions. Typically, deaerated MeCN solutions of anthracene (1.2×10^{-3} M) and $[Ru(bpy)_3](PF_6)_3$ (7.0×10^{-3} M) were transferred to the spectrophotometric cell by means of a glass syringe which had earlier been purged with a stream of argon. Both the decay of anthracene radical cation produced in electron transfer from anthracene to $[Ru(bpy)_3]^{3+}$ and the formation of $[Ru(bpy)_3]^{2+}$ associated with the six-electron oxidation of anthracene in deaerated MeCN at 298 K were monitored by following a decrease in absorbance at 720 nm ($\epsilon = 8.60 \times 10^3$ M^{-1} cm^{-1}) due to anthracene radical cation and an increase in absorbance at 450 nm ($\epsilon = 1.38 \times 10^4$ M^{-1} cm^{-1})[25] due to $[Ru(bpy)_3]^{2+}$. The ϵ values of the radical cations of anthracene and 9-alkylanthracene were determined from the initial absorbances due to the radical cations at time zero by taking account of the mixing time. The second-order plots of $(A_\infty - A)^{-1}$ vs time (A_∞ and A are the final absorbance and the absorbance at the reaction time, respectively) were linear with the correlation coefficient $\rho > 0.999$. Second-order rate constants (k_{obs}) were determined by a least-squares curve fit using a Macintosh personal computer. In each case, it was confirmed that the k_{obs} values derived from at least five independent measurements agreed within an experimental error of ±5%.

Cyclic Voltammetry. The fast cyclic voltammetry measurements of anthracene and 9-alkylanthracene in deaerated MeCN containing 0.1 M TBAP as supporting electrolyte were performed on a Fuso model HECS 972 potentiostat−galvanostat by using the platinum microelectrode (10 μm i.d.) at the sweep rate of 2000 V s^{-1}. The counter electrodes were platinum, while $Ag/AgNO_3$ (0.01 M) was used as the reference electrode. All potentials are reported as V vs SCE. The one-electron oxidation potential (E^0_{ox}) value of ferrocene used as a standard is 0.37 V vs SCE in MeCN under our solution conditions.[30]

ESR Measurements. The ESR measurements were performed on a JEOL X-band spectrometer (JES-RE1XE). Deaerated MeCN solutions of various concentrations of 9,10-dimethylanthracene and $[Fe(phen)_3](ClO_4)_3$ under atmospheric pressure of nitrogen were mixed in the capillary cell by using a JEOL JES-SM-1 rapid mixing flow apparatus. The ESR spectra were recorded under nonsaturating microwave power conditions. The magnitude of modulation was chosen to optimize the resolution and the signal-to-noise (*S*/*N*) ratio of the observed spectra. The *g* values were calibrated with a Mn^{2+} marker and hyperfine splitting values were determined by computer simulation using an Calleo ESR version 1.2 program coded by Calleo Scientific Software Publishers on a Macintosh personal computer.

Results and Discussion

Multielectron Oxidation of Anthracenes. The one-electron reduction potential of $[Ru(bpy)_3](PF_6)_3$ ($E^0_{red} = 1.24$ V)[31] in MeCN is more positive than the one-electron oxidation potential of anthracene in the same solvent ($E^0_{ox} = 1.19$ V). Thus, electron transfer from anthracene to $[Ru(bpy)_3](PF_6)_3$ is energetically feasible. UV−visible spectra observed after the oxidation of anthracene with different concentrations of $[Ru(bpy)_3]^{3+}$ are shown in Figure 1 where the absorption band at 450 nm due to $[Ru(bpy)_3]^{2+}$ increases upon successive addition of $[Ru(bpy)_3]^{3+}$ to a deaerated MeCN solution containing anthracene (2.1×10^{-5} M) and H_2O (7.0×10^{-3} M). The spectral titration (inset of Figure 1) reveals that 6 equiv of $[Ru(bpy)_3]^{3+}$ are consumed to oxidize 1 equiv of anthracene. In fact, anthraquinone, which is the six-electron oxidized product of anthracene, is isolated (91%

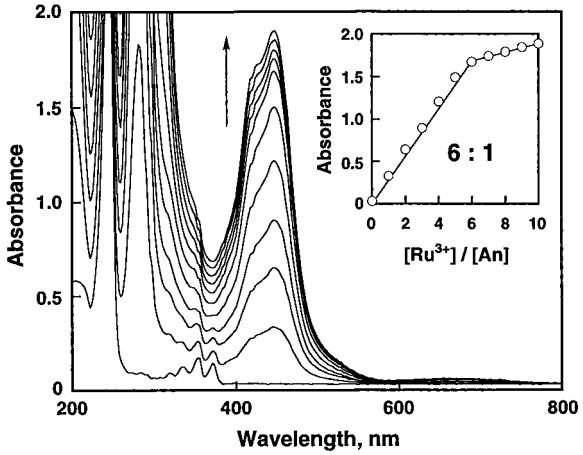

Figure 1. Spectral changes observed upon addition of $[Ru(bpy)_3]^{3+}$ (2.1×10^{-5}, 4.3×10^{-5}, 6.4×10^{-5}, 8.5×10^{-5}, 1.1×10^{-4}, 1.3×10^{-4}, 1.5×10^{-4}, 1.7×10^{-4}, 1.9×10^{-4}, and 2.1×10^{-4} M) to an MeCN solution of An (2.1×10^{-5} M). Inset: plot of the absorbance at 450 nm vs $[Ru(bpy)_3]^{3+}$/[An].

yield, see Experimental Section) after the oxidation of anthracene with 6 equiv of $[Ru(bpy)_3]^{3+}$. The product was identified by the ^{1}H NMR spectrum and mass spectroscopy. Thus, the stoichiometry of the oxidation of anthracene with $[Ru(bpy)_3]^{3+}$ is given by eq 1.

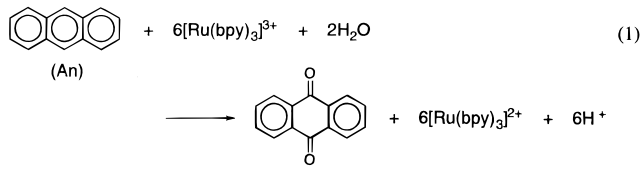

(1)

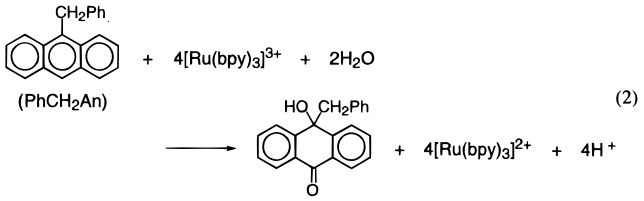

(2)

When anthracene is replaced by 9-benzylanthracene, the ring oxidation occurs to yield the four-electron oxidized species, 10-benzyl-10-hydroxy-9(10H)-anthracenone as shown in eq 2. The product was also identified by the ^{1}H NMR spectrum and mass spectroscopy. The oxidation of 9-ethylanthracene (EtAn) also yields the 10-ethyl-10-hydroxy-9(10H)-anthracenone (see Experimental Section).

Decay Kinetics of Anthracene Radical Cations. Mixing an MeCN solution ($[H_2O] = 7.0 \times 10^{-3}$ M) of anthracene (An: 6.0×10^{-4} M) with 6 equiv of $[Ru(bpy)_3](PF_6)_3$ (3.6×10^{-3} M) in a stopped-flow spectrometer results in an instant appearance of a new absorption band at $\lambda_{max} = 720$ nm due to anthracene radical cation ($An^{\bullet+}$)[32] as shown in Figure 2. The decay of absorbance at 720 nm due to $An^{\bullet+}$ coincides with an appearance of absorbance at 450 nm due to 5 equiv of $[Ru(bpy)_3]^{2+}$ following the initial rapid increase due to formation of 1 equiv of $[Ru(bpy)_3]^{2+}$, accompanied by the formation of $An^{\bullet+}$.[33] Both the rates of decay of $An^{\bullet+}$ and the formation of 5 equiv of $[Ru(bpy)_3]^{2+}$ obeys the second-order kinetics as shown in the linear plots of $(A_\infty - A)^{-1}$ vs time (see insets in Figure 3; A is absorbance at time t and A_∞ is the final absorbance after the reaction). After the complete decay of anthracene radical cation, there is no further increase in absorbance due to $[Ru(bpy)_3]^{2+}$. It should be emphasized that the consumption of 5 equiv of $[Ru(bpy)_3]^{3+}$ coincides exactly with the decay of anthracene radical cation derived from 1 equiv of anthracene. Thus, the kinetics of decay of $An^{\bullet+}$ and that of formation of $[Ru(bpy)_3]^{2+}$ are given by eqs 3 and 4, where $[Ru(bpy)_3]^{3+/2+}$ is represented as

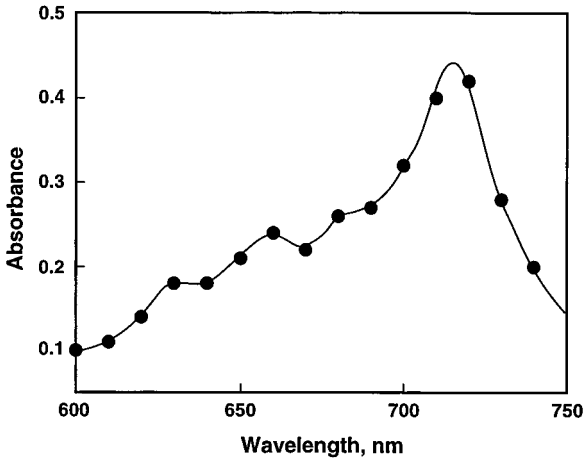

Figure 2. Transient absorption spectrum of $An^{\bullet+}$ formed in the electron-transfer oxidation of An (6.0×10^{-4} M) with $[Ru(bpy)_3]^{3+}$ (5.0×10^{-3} M) in deaerated MeCN.

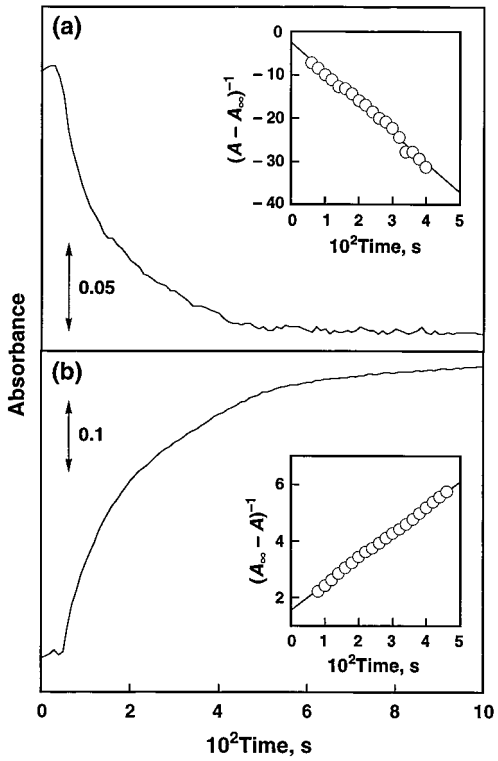

Figure 3. Time course of the absorption changes (a) at 720 nm due to decay of $An^{\bullet+}$ and (b) at 450 nm due to formation of $[Ru(bpy)_3]^{2+}$ in the electron-transfer oxidation of An (6.0×10^{-4} M) with $[Ru(bpy)_3]^{3+}$ (3.6×10^{-3} M) in MeCN at 298 K. Inset: the second-order plot.

$$-d[An^{\bullet+}]/dt = k_{obs}[An^{\bullet+}]^2 \quad (3)$$

$$d[Ru^{2+}]/dt = (k_{obs}/5)\{[Ru^{2+}]_\infty - [Ru^{2+}]\}^2 = 5k_{obs}[An^{\bullet+}]^2 \quad (4)$$

$Ru^{3+/2+}$ and $[Ru^{2+}]_\infty$ is the final concentration of $[Ru(bpy)_3]^{2+}$ which is equal to $5[An]_0$ (the subscript 0 denotes the initial

TABLE 1: Absorption Maxima (λ_{max}) and Extinction Coefficients (ϵ_{max}) of 9-Alkylanthracene Radical Cations ($RAn^{\bullet+}$), the One-Electron Oxidation Potentials (E^0_{ox}) of RAn, the Observed Second-Order Rate Constants (k_{obs}) for the Decay of $RAn^{\bullet+}$ Generated by Electron-Transfer Oxidation of RAn with $[Ru(bpy)_3](PF_6)_3$ (2.0×10^{-2} M), and Rate Constants (k_1) for Disproportionation Reaction of $RAn^{\bullet+}$ in Deaerated MeCN Containing 7.0×10^{-3} M H_2O at 298 K

RAn	λ_{max}[a] nm	$10^{-3}\epsilon_{max}$[b] M^{-1} cm^{-1}	E^0_{ox} (vs SCE) V	k_{obs}[b] M^{-1} s^{-1}	k_1[b] M^{-1} s^{-1}
An	720	8.6	1.19	1.1×10^6	1.1×10^6
$PhCH_2An$	720	7.0	1.20	1.3×10^5	
EtAn	700	8.0	1.14	1.4×10^5	1.6×10^5
Me_2An	680	8.6	1.14	1.5×10^3	2.4×10^3

[a] The experimental error is ±10 nm. [b] The experimental error is ±10%.

concentration). The observed second-order rate constant (k_{obs}) derived from eq 3 (1.2×10^{-6} M^{-1} s^{-1}) agrees well with that derived from eq 4 (1.3×10^{-6} M^{-1} s^{-1}). Such an agreement indicates strongly that the rate-determining step for the six-electron oxidation of anthracene is the bimolecular reaction of anthracene radical cation.

Similar transient absorption spectra of radical cations derived alkylanthracenes are detected in the reactions of alkylanthracenes with $[Ru(bpy)_3](PF_6)_3$. The absorption maxima (λ_{max}) and the extinction coefficients (ϵ_{max}) of radical cations of anthracenes are listed in Table 1, together with the one-electron oxidation potentials of anthracites determined by the fast cyclic voltammograms (see Experimental Section). In each case, both the rates of decay of alkylanthracene radical cation and the formation of $[Ru(bpy)_3]^{2+}$ obeys the second-order kinetics and the k_{obs} values for the multielectron oxidation of anthracene (An) and alkylanthracenes (RAn) with $[Ru(bpy)_3]^{3+}$ (2.0×10^{-2} M) in MeCN containing 7.0×10^{-3} M H_2O at 298 K are listed in Table 1. The k_{obs} value of $RAn^{\bullet+}$ decreases in the order: An > $PhCH_2An$ ≅ EtAn > Me_2An.

The second-order kinetics for the decay of $RAn^{\bullet+}$ holds at various concentrations of $[Ru(bpy)_3]^{3+}$, [RAn], and H_2O. The k_{obs} values for the decay of anthracene radical cation in the oxidation of anthracene with more than 6 equiv of $[Ru(bpy)_3]^{3+}$ and with less than 1 equiv of $[Ru(bpy)_3]^{3+}$ are independent of changes in the concentrations of $[Ru(bpy)_3]^{3+}$ and anthracene as shown in parts a and b of Figure 4, respectively. The k_{obs} value with excess anthracene is 6 times larger than that with excess $[Ru(bpy)_3]^{3+}$ (eq 5).

$$k_{obs}([An] > [Ru^{3+}]) = 6k_{obs}([Ru^{3+}] > 6[An]) \qquad (5)$$

The decay of $An^{\bullet+}$ is accelerated by the presence of H_2O. The k_{obs} value increases linearly with an increase in $[H_2O]$ as shown in Figure 5. When H_2O is replaced by D_2O, the same k_{obs} values are obtained at the same water concentrations ($k_{obs}(H_2O) = 3.20 \times 10^6$ M^{-1} s^{-1}; $k_{obs}(D_2O) = 3.17 \times 10^6$ M^{-1} s^{-1} at $[An] = 6.0 \times 10^{-5}$ M; $[Ru(bpy)_3]^{3+} = 6.0 \times 10^{-5}$ M; [H_2O or D_2O] $= 2.5 \times 10^{-2}$ M). Thus, there is no kinetic deuterium isotope effect of water for the decay of anthracene radical cation.

When anthracene is replaced by the deuterated compound, anthracene-d_{10}, the larger k_{obs} value (1.39×10^6 M^{-1} s^{-1}) is obtained for the decay of the radical cation in the oxidation of anthracene-d_{10} (6.0×10^{-4} M^{-1} s^{-1}) with $[Ru(bpy)_3]^{3+}$ (5.0×10^{-3} M) as compared to the corresponding k_{obs} value of anthracene (9.85×10^5 M^{-1} s^{-1}). Such inverse kinetic isotope effects ($k_H/k_D = 0.71$) may be due to the hybridization change,

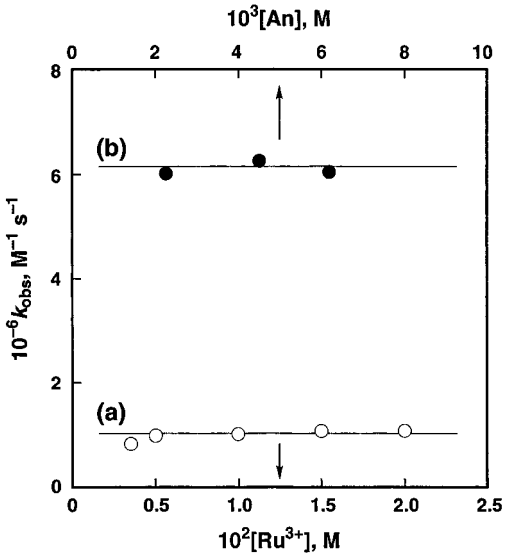

Figure 4. Plots of (a) k_{obs} vs $[Ru^{3+}]$ (○) for the decay of $An^{\bullet+}$ formed in the electron-transfer oxidation of An (6.0×10^{-4} M) with $[Ru(bpy)_3]^{3+}$ and (b) k_{obs} vs [An] (●) for the decay of $An^{\bullet+}$ formed in the electron-transfer oxidation of An with $[Ru(bpy)_3]^{3+}$ (5.6×10^{-4}) in deaerated MeCN at 298 K.

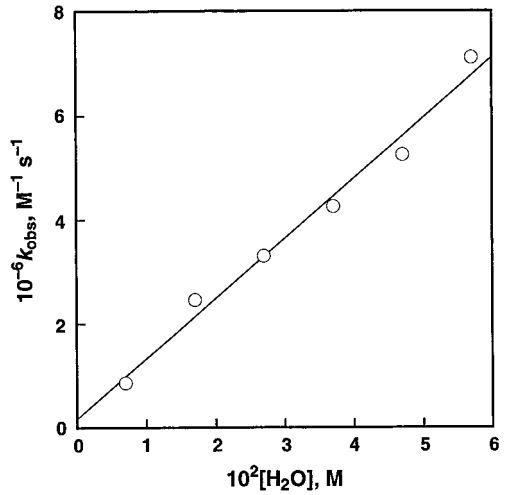

Figure 5. Plot of k_{obs} vs $[H_2O]$ for the decay of $An^{\bullet+}$ formed in the electron-transfer oxidation of An (6.0×10^{-4} M) with $[Ru(bpy)_3]^{3+}$ (1.0×10^{-2} M) in deaerated MeCN at 298 K.

sp^2 to sp,[3,9d,34] that occurs during the decay of the radical cation as discussed later.

The k_{obs} value for the decay of 9-ethylanthracene radical cation ($EtAn^{\bullet+}$) as well as 9,10-dimethylanthracene radical cation ($Me_2An^{\bullet+}$) increases with an increase in the $[Ru(bpy)_3]^{3+}$ concentration to reach a constant value as shown in Figure 6 (part a and b, respectively). In the case of 9-benzylanthracene ($PhCH_2An$), however, the k_{obs} value increases linearly with an increase in the $[Ru(bpy)_3]^{3+}$ concentration exhibiting no saturation up to 2.0×10^{-2} M as shown in Figure 7. Since the k_{obs} value of $PhCH_2An$ is relatively small as compared with the corresponding value of An (see Table 1), the acceleration effect of H_2O on k_{obs} can be examined in the presence of much higher concentrations of H_2O than the case of An (Figure 5). The k_{obs} value increases with an increase in $[H_2O]$ to exhibit first-order dependence on $[H_2O]$ at low concentrations, changing to second-order dependence at high concentrations, as shown in Figure 8. When H_2O is replaced by D_2O, the same k_{obs} values are obtained at the same water concentrations ($k_{obs}(H_2O) = 2.1 \times 10^4$ M^{-1} s^{-1}; $k_{obs}(D_2O) = 2.0 \times 10^4$ M^{-1} s^{-1} at $[PhCH_2An] = 7.0 \times$

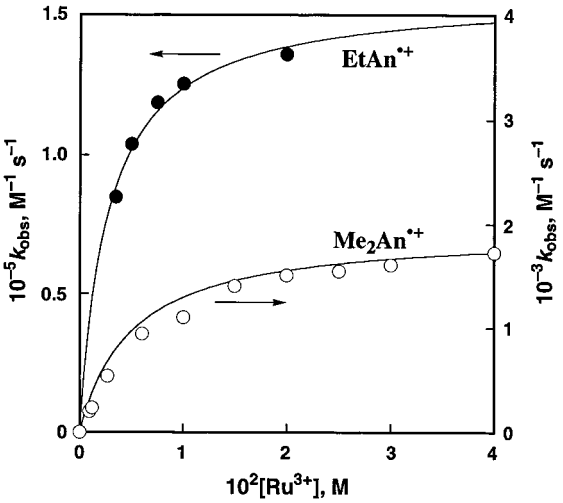

Figure 6. Plots of k_{obs} vs $[Ru^{3+}]$ for the decay of $EtAn^{\bullet+}$ (●) and $Me_2An^{\bullet+}$ (○) formed in the electron-transfer oxidation of EtAn (6.0×10^{-4} M) and Me_2An (6.0×10^{-4} M), respectively, with $[Ru(bpy)_3]^{3+}$ in deaerated MeCN at 298 K.

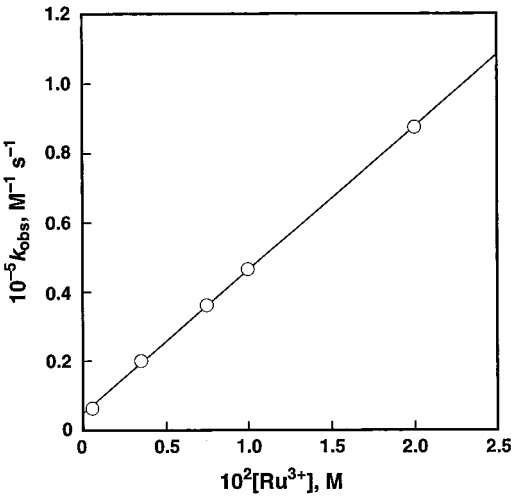

Figure 7. Plot of k_{obs} vs $[Ru^{3+}]$ for the decay of $PhCH_2An^{\bullet+}$ formed in the electron-transfer oxidation of $PhCH_2An$ (6.0×10^{-4} M) with $[Ru(bpy)_3]^{3+}$ in deaerated MeCN at 298 K.

10^{-4} M; $[Ru(bpy)_3]^{3+} = 5.6 \times 10^{-4}$ M; [H_2O or D_2O] = 0.05 M). Thus, there is no kinetic deuterium isotope effect of water for the decay of $PhCH_2An^{\bullet+}$ as the case of $An^{\bullet+}$.

Mechanisms of Multielectron Oxidation of Anthracenes. Since the rate-determining step for the multielectron oxidation of anthracenes with $[Ru(bpy)_3]^{3+}$ is found to be the bimolecular reactions of anthracene radical cations produced in the initial electron transfer from anthracenes to $[Ru(bpy)_3]^{3+}$, the decay kinetics of anthracene radical cations by itself provides no direct information on the mechanisms of the product-forming steps. Nonetheless, such finding on the rate-determining step for the multielectron oxidation of anthracenes indicates that the decay of anthracene radical cations results in formation of products which are rapidly oxidized to lead to the final multielectron oxidized products. The detailed kinetic results combined with the product analyses provide valuable information on the overall mechanism for the multielectron oxidation of anthracenes, since any mechanism should explain all the following experimental observations:

(1) the six-electron oxidation of anthracene to anthraquinone (Figure 1, eq 1);

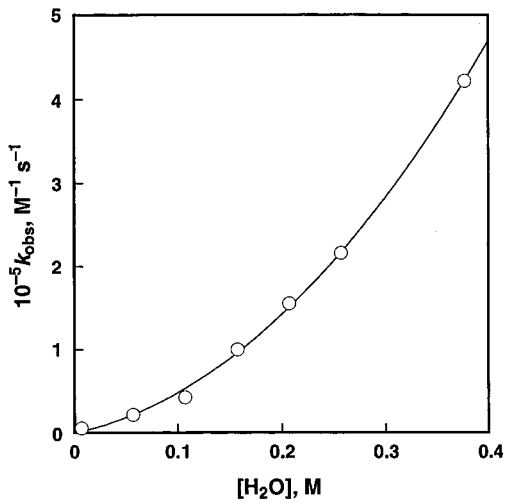

Figure 8. Plots of k_{obs} vs $[H_2O]$ for the decay of $PhCH_2An^{\bullet+}$ formed in the electron-transfer oxidation of $PhCH_2An$ (7.0×10^{-5} M) with $[Ru(bpy)_3]^{3+}$ (7.0×10^{-4} M) in deaerated MeCN at 298 K.

SCHEME 1

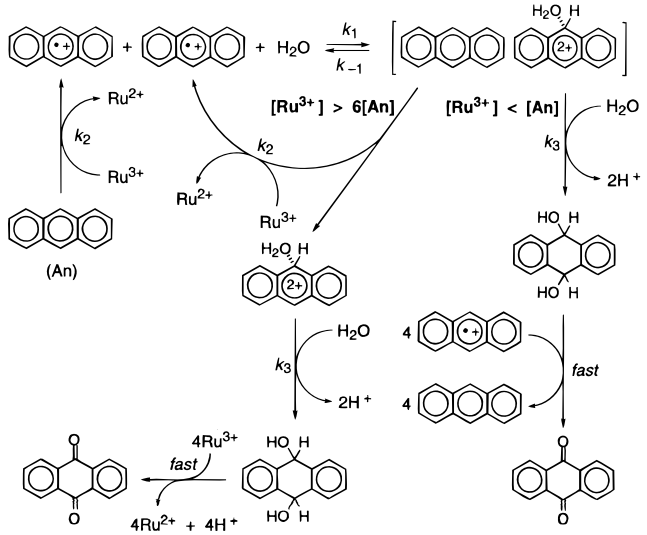

(2) the four-electron oxidation of 9-alkylanthracene to 10-alkyl-10-hydroxy-9(10H)-anthracenone (eq 2);

(3) the second-order kinetics for both the decay of anthracene radical cation (eq 3) and formation of $[Ru(bpy)]^{2+}$ (eq 4) and the relation, $d[Ru^{2+}]/dt = -5d[An^{\bullet+}]/dt$ (Figure 3);

(4) the k_{obs} value with excess anthracene being 6 times larger than that with excess $[Ru(bpy)]^{3+}$ (Figure 4, eq 5);

(5) the dependence of k_{obs} on $[Ru^{3+}]$ (Figures 4, 6, 7);

(6) the accelerating effects of H_2O on the k_{obs} values (Figures 5 and 8);

(7) the absence of kinetic deuterium isotope effects of D_2O on k_{obs};

(8) the observation of inverse kinetic isotope effects of anthracene-d_{10} on k_{obs}

For the sake of clarifying and better understanding of this study, we first present the reaction mechanism of the six-electron oxidation of anthracene with $[Ru(bpy)_3]^{3+}$ as shown in Scheme 1 and then discuss how this mechanism can explain all the experimental observations summarized above.

The six-electron oxidation of anthracene (An) is started by a rapid electron transfer from An to $[Ru(bpy)_3]^{3+}$ to produce the radical cation ($An^{\bullet+}$). The electron-transfer disproportionation between $An^{\bullet+}$ occurs to give An and An^{2+}. The free energy

change of electron transfer between $An^{\bullet+}$ (ΔG^0_{et}) in the absence of H_2O is given by eq 6,

$$\Delta G^0_{et} = F(E^0_{ox} - E^0_{red}) \quad (6)$$

where E^0_{ox} is the one-electron oxidation potential of $An^{\bullet+}$, E^0_{red} is the one-electron reduction potential of $An^{\bullet+}$ (E^0_{red}) which is equivalent to the one-electron oxidation potential of An, and F is the Faraday constant. Since the one-electron oxidation potential of $An^{\bullet+}$ is more positive than the one-electron oxidation potential of An,[35] the electron transfer between $An^{\bullet+}$ is endergonic ($\Delta G^0_{et} > 0$). In such a case, the electron transfer (k_1) should be followed by rapid back electron transfer (k_{-1}) to regenerate the product pair (Scheme 1). In the present case, however, electron transfer from An to $[Ru(bpy)_3]^{3+}$ is energetically feasible (vide infra), and thereby the electron-transfer disproportionation of $An^{\bullet+}$ to give An and An^{2+} should be followed by a fast electron transfer from An to $[Ru(bpy)_3]^{3+}$ (k_2) to reproduce $An^{\bullet+}$. Since An^{2+} is a strong electrophile, An^{2+} may react rapidly with H_2O (k_3) to produce the dihydroxy adduct. This can be rapidly oxidized to anthraquinone by 4 equiv of $[Ru(bpy)_3]^{3+}$ when more than 6 equiv of $[Ru(bpy)_3]^{3+}$ are used for the oxidation of An (Scheme 1).

When less than 1 equiv of $[Ru(bpy)_3]^{3+}$ is used to start the oxidation of An, $[Ru(bpy)_3]^{3+}$ is consumed completely in the initial electron transfer from An to $[Ru(bpy)_3]^{3+}$ to generate $An^{\bullet+}$. In such a case, the dihydroxy adduct formed by the reaction of An^{2+} with H_2O may be oxidized to anthraquinone by 4 equiv of $An^{\bullet+}$ (Scheme 1).

According to Scheme 1, the decay rate of $An^{\bullet+}$ in the presence of more than 6 equiv of $[Ru(bpy)_3]^{3+}$ is expressed by eq 7 as a function of $[Ru^{3+}]$. The rate of formation of $[Ru(bpy)_3]^{2+}$ is given by eq 8.

$$-d[An^{\bullet+}]/dt = k_1(k_2[Ru^{3+}] + 2k_3)/(k_{-1} + k_3 + k_2[Ru^{3+}])[An^{\bullet+}]^2 \quad (7)$$

$$d[Ru^{2+}]/dt = k_1(5k_2[Ru^{3+}] + 4k_3)/(k_{-1} + k_3 + k_2[Ru^{3+}])[An^{\bullet+}]^2 \quad (8)$$

Under the conditions that $[Ru^{3+}] \gg k_3 \gg k_{-1}$, eqs 7 and 8 are reduced to eqs 9 and 10, respectively. Equations 9 and 10 agree with the experimental observations in eqs 3 and 4, respectively, where k_{obs} corresponds to the rate constant of electron-transfer disproportionation (k_1).

$$-d[An^{\bullet+}]/dt = k_1[An^{\bullet+}]^2 \quad (9)$$

$$d[Ru^{2+}]/dt = 5k_1[An^{\bullet+}]^2 = -5d[An^{\bullet+}]/dt \quad (10)$$

When less than 1 equiv of $[Ru(bpy)_3]^{3+}$ is used to start the six-electron oxidation of An, no $[Ru(bpy)_3]^{3+}$ is left after the electron transfer from An to $[Ru(bpy)_3]^{3+}$ to produce $An^{\bullet+}$. In such a case, 4 equiv of $An^{\bullet+}$ is rapidly consumed following the formation of the dihydroxy adduct (Scheme 1). Then, the decay rate of $An^{\bullet+}$ in the presence of less than 1 equiv of $[Ru(bpy)_3]^{3+}$ is expressed by eq 11. Since $k_3 \gg k_{-1}$ (vide supra), the observed second-order rate constant k_{obs} is expressed by eq 12 which agrees with the experimental observation in Figure 4 (eq 5), where k_{obs} ($[Ru^{3+}] > 6[An]$) $= k_1$ (vide supra).

$$-d[An^{\bullet+}]/dt = 6k_1k_3/(k_{-1} + k_3)[An^{\bullet+}]^2 \quad (11)$$

$$(k_{obs}([An] > [Ru^{3+}]) = 6k_1 \quad (12)$$

SCHEME 2

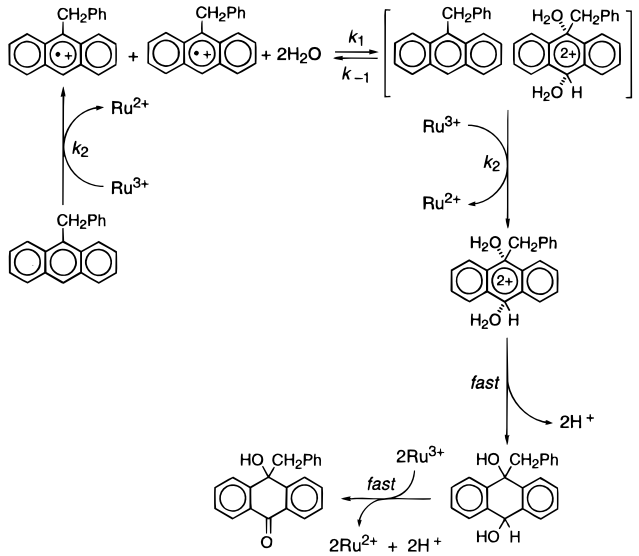

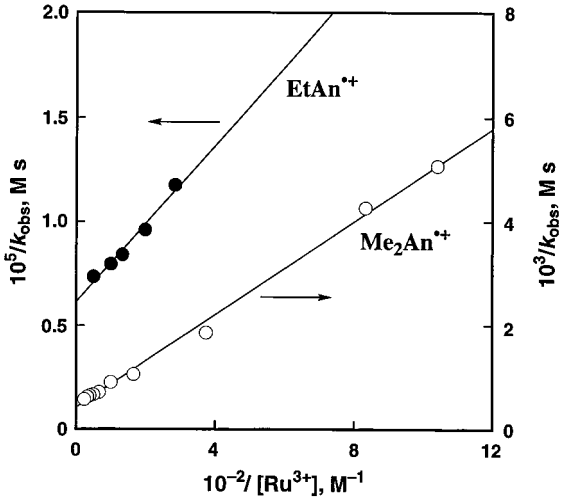

Figure 9. Plots of $1/k_{obs}$ vs $1/[Ru^{3+}]$ for the decay of $EtAn^{\bullet+}$ (●) and $Me_2An^{\bullet+}$ (○) formed in the electron-transfer oxidation of EtAn (6.0×10^{-4} M) and Me_2An (6.0×10^{-4} M), respectively, with $[Ru(bpy)_3]^{3+}$ in deaerated MeCN at 298 K.

The four-electron oxidation of RAn (R = Et and $PhCH_2$) with more than 4 equiv of $[Ru(bpy)_3]^{3+}$ may also proceed via the electron-transfer disproportionation of $RAn^{\bullet+}$ as shown in Scheme 2 for the case of $PhCH_2An$. In this case, the dihydroxy adduct of $PhCH_2An^{2+}$ is further oxidized to 10-alkyl-10-hydorxy-9(10H)anthracenone by 2 equiv of $[Ru(bpy)_3]^{3+}$. The involvement of two H_2O molecules in the electron-transfer disproportionation of $PhCH_2An^{\bullet+}$ in Scheme 2 will be discussed in relation with the catalytic effect of H_2O in the next section.

According to Scheme 2, the decay rate of $RAn^{\bullet+}$ is also expressed as a function of $[Ru^{3+}]$ by eq 13, and the observed second-order rate constant k_{obs} is given by eq 8 which is rewritten by eq 14.

$$k_{obs} = k_1k_2[Ru^{3+}]/(k_{-1} + k_2[Ru^{3+}]) \quad (13)$$

$$k_{obs}^{-1} = k_1^{-1} + (k_1k_2[Ru^{3+}]/k_{-1})^{-1} \quad (14)$$

A linear correlation between k_{obs}^{-1} and $[Ru^{3+}]^{-1}$ predicted by eq 14 is shown in Figure 9 for the k_{obs} values of $EtAn^{\bullet+}$ and $Me_2An^{\bullet+}$. From the intercepts of the linear plots are obtained the k_1 values, which are listed in Table 1. The k_1 value of $An^{\bullet+}$,

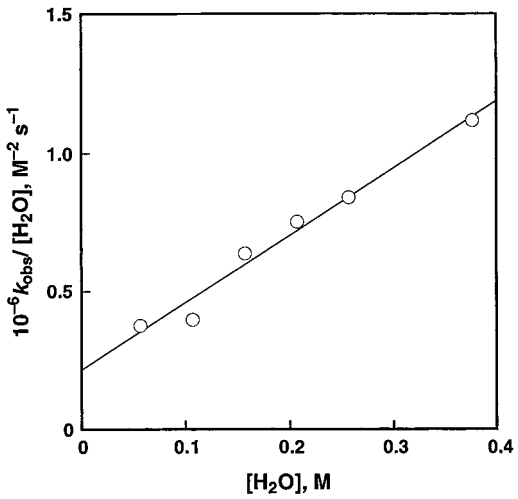

Figure 10. Plot of $k_{obs}/[H_2O]$ vs $[H_2O]$ for the decay of $PhCH_2An^{\bullet+}$ formed in the electron-transfer oxidation of $PhCH_2An$ (7.0×10^{-5} M) with $[Ru(bpy)_3]^{3+}$ (7.0×10^{-4} M) in deaerated MeCN at 298 K.

which is obtained as a constant value in Figure 4, is also listed in Table 1. In the case of $PhCH_2An^{\bullet+}$, the k_{-1} value may be much larger than the $k_2[Ru^{3+}]$ values under the experimental conditions in Figure 7, where the k_{obs} value increases linearly with increase in $[Ru^{3+}]$.

Catalysis of Water on Electron-Transfer Disproportionation. The first-order and second-order dependence of k_{obs} of $PhCH_2An^{\bullet+}$ on $[H_2O]$ in Figure 8 may be explained by the complex formation of $PhCH_2An^{2+}$ with one and two H_2O molecules as shown in Scheme 2. The complex formation of $PhCH_2An^{2+}$ and H_2O should result in the negative shift of the one-electron oxidation potential of $PhCH_2An^{\bullet+}$ (E_{ox}). The Nernst equation may be given by eq 15, where E^0_{ox} is the one-electron oxidation potential of $PhCH_2An^{\bullet+}$ in the absence of H_2O,

$$E_{ox} = E^0_{ox} - (2.3RT/F) \log K_1[H_2O](1 + K_2[H_2O]) \quad (15)$$

and $K_1[H_2O] \gg 1$. From eq 15 is derived the dependence of the rate constant of electron-transfer disproportionation (k_1) on $[H_2O]$ as given by eq 16, where k_0 is the rate constant in the absence of H_2O. Since k_{obs} is proportional to k_1 (eq 13), the validity to eq 16 is confirmed by

$$(k_1 - k_0)/[H_2O] = k_0K_1(1 + K_2[H_2O]) \quad (16)$$

the linear plot of $k_{obs}/[H_2O]$ vs $[H_2O]$ for the data in Figure 8 as shown in Figure 10. The absence of the kinetic deuterium isotope effect of water (Figure 8) is also consistent with Scheme 2 where no cleavage of O−H bond is involved in the water-accelerated electron-transfer reaction between $PhCH_2An^{\bullet+}$.

The second-order dependence of k_{obs} of $PhCH_2An^{\bullet+}$ on $[H_2O]$ may be alternatively explained by the bimolecular reactions of $PhCH_2An^{\bullet+}$ which forms a complex with H_2O (eq 17). In such a case, the bimolecular reaction between $PhCH_2An^{\bullet+}-H_2O$ complexes (eq 18) would be responsible for the second-order dependence on $[H_2O]$.

$$PhCH_2An^{\bullet+} + H_2O \rightleftarrows PhCH_2An^{\bullet+}-H_2O \quad (17)$$

$$2(PhCH_2An^{\bullet+}-H_2O) \rightarrow PhCH_2An^{2+}-2H_2O + PhCH_2An \quad (18)$$

However, the complex formation of $PhCH_2An^{\bullet+}$ with H_2O may result in an increase in the donor ability but a decrease in the electron acceptor ability. In such a case, the reaction between $PhCH_2An^{\bullet+}-H_2O$ and $PhCH_2An^{\bullet+}$ (the first-order dependence of k_{obs} on $[H_2O]$) would be faster than the reaction between the $PhCH_2An^{\bullet+}-H_2O$ complexes (the second-order dependence of k_{obs} on $[H_2O]$). Thus, the second-order acceleration of the rate with an increase in $[H_2O]$ can only be explained by the complex formation of $PhCH_2An^{2+}$ with 2 equiv of H_2O. Although the complex formation occurs after the electron transfer between $PhCH_2An^{\bullet+}$, the 1:1 and 1:2 complex formation of $PhCH_2An^{2+}$ with H_2O causes a decrease in the free energy change of electron transfer because of the negative shift of the oxidation potential of $PhCH_2An^{\bullet+}$ (eq 15). This results in the first-order and second-order acceleration of the rate of electron transfer (eq 16). Such a first-order and second-order catalysis on an electron-transfer reaction has been well documented for a Mg^{2+}-catalyzed electron-transfer reaction from a one-electron reductant to *p*-benzoquinone, which is ascribed to the 1:1 and 1:2 complex formation of semiquinone radical cation and Mg^{2+}.[36] Such catalysis of metal ions on both thermal and photoinduced electron-transfer reactions has recently been reviewed in comparison with catalysis on polar reactions.[37,38]

The electron-transfer disproportionation of $An^{\bullet+}$ may also be accelerated by the 1:1 and 1:2 complex formation of An^{2+} with H_2O although the observed k_{obs} values of $An^{\bullet+}$ in the presence of large concentrations of H_2O, where the k_{obs} value of $An^{\bullet+}$ may exhibit the second-order dependence on $[H_2O]$, were so rapid as to fall outside the stopped-flow range.

The absence of kinetic deuterium isotope effect of D_2O on k_{obs} for the decay of $An^{\bullet+}$ (vide supra) indicates that no oxygen−hydrogen bond cleavage is involved in the water-accelerated electron-transfer disproportionation of $An^{\bullet+}$. On the other hand, the observation of the inverse secondary kinetic isotope effect ($k_H/k_D = 0.71$, vide supra) suggests that the interaction of An^{2+} with H_2O results in the hybridization change from sp^2 to sp^3 as shown in Scheme 1.[9d,34] As suggested by Shaik and Pross,[15] such a strong interaction between a radical cation and a nucleophile may be "forbidden" but the "allowed" interaction of the dication with H_2O may be strong enough to cause the hybridization change in the transition state of electron transfer.

Evaluation of Rate Constants of Electron-Transfer Disproportionation. Since the multielectron oxidation of An and RAn proceeds via the rate-determining electron-transfer disproportionation of the corresponding radical cations as shown in Schemes 1 and 2, respectively, it is required to evaluate the free energy change of electron transfer between the radical cations (ΔG^0_{et}) in order to understand the difference in the reactivity of An and RAn. The ΔG^0_{et} values in the absence of H_2O can be obtained from the E^0_{ox} and E^0_{red} values of $An^{\bullet+}$ and $RAn^{\bullet+}$ (eq 6). The E^0_{red} values of $An^{\bullet+}$ and $RAn^{\bullet+}$ are determined as the first one-electron oxidation potentials of An and RAn as listed in Table 1. However, it is extremely difficult to determine the E^0_{ox} values of $An^{\bullet+}$ and $RAn^{\bullet+}$ because of instability of the corresponding dications (An^{2+} and RAn^{2+}). When the strongly reactive 9- and 10-positions of anthracene are protected by CH_3 substitution, a reversible cyclic voltammogram of Me_2An is obtained for the first and second oxidation step.[35] Thus, the $\Delta G^0_{et}/F$ value for the electron-transfer disproportionation of $Me_2An^{\bullet+}$ is obtained from the difference in the first and second oxidation potentials as 0.44 V.[35]

The dependence of the activation free energy $\Delta G^{\ddagger}$ of electron transfer on ΔG^0_{et} has been well established by Marcus and follows the relationship shown in eq 19,

$$\Delta G^{\ddagger} = (\lambda/4)(1 + \Delta G^0_{et}/\lambda)^2 \quad (19)$$

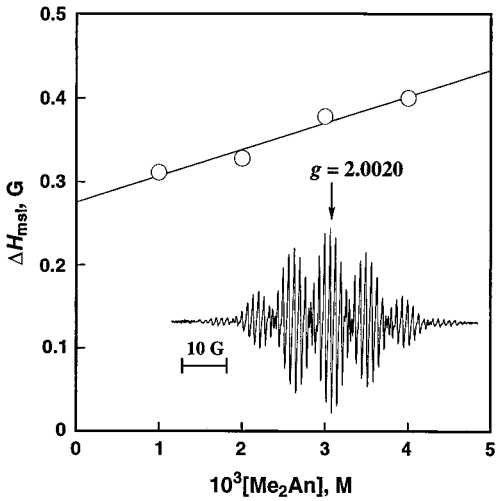

Figure 11. Plot of [Me_2An] vs ΔH_{msl} of ESR spectra of $Me_2An^{\bullet+}$ in MeCN at 298 K. Inset: ESR spectrum of $Me_2An^{\bullet+}$ generated in the electron-transfer oxidation of Me_2An (1.0×10^{-2} M) with $[Fe(phen)_3]^{3+}$ (1.0×10^{-2} M) in MeCN at 298 K.

where λ is the reorganization energy of the electron-transfer reaction.[39] The $\Delta G^{\ddagger}$ values are obtained from the rate constant of electron transfer (k_{et}) and the diffusion rate constant (k_{diff}) using eq 20, where Z is the collision frequency taken as 1×10^{11} M^{-1} s^{-1}, F is the Faraday constant, the k_{diff} value in MeCN is 2.0×10^{10} M^{-1} s^{-1} and the other notations are conventional.

$$\Delta G^{\ddagger} = (2.3RT/F) \log[Z(k_{et}^{-1} - k_{diff}^{-1})] \qquad (20)$$

To determine the self-exchange rate constant between $Me_2An^{\bullet+}$ and Me_2An (eq 21),

$$Me_2An + Me_2An^{\bullet+} \overset{k_{ex}}{\rightleftharpoons} Me_2An^{\bullet+} + Me_2An \qquad (21)$$

the ESR spectra of $Me_2An^{\bullet+}$ produced by electron transfer from Me_2An to $[Ru(bpy)_3]^{3+}$ were measured in the presence of various concentrations of Me_2An in MeCN (inset in Figure 11).[40] The maximum slope line width (ΔH_{msl}) of the ESR spectrum of $Me_2An^{\bullet+}$ increases linearly with an increase in the concentration of Me_2An as shown in Figure 11. The rate constants (k_{ex}) of the electron exchange reactions between $Me_2An^{\bullet+}$ and Me_2An (eq 19) were determined as 5.0×10^8 M^{-1} s^{-1} using eq 22,

$$k_{ex} = 1.52 \times 10^7(\Delta H_{msl} - \Delta H^0_{msl})/\{(1 - P_i)[Me_2An]\} \qquad (22)$$

where ΔH_{msl} and ΔH^0_{msl} are the maximum slope line widths of the ESR spectra in the presence and absence of Me_2An, respectively, and P_i is a statistical factor.[41] The reorganization energies (λ) of the electron-transfer reaction is obtained as 12.5 kcal mol^{-1} from the k_{ex} values using eq 23 ($Z = 10^{11}$ M^{-1} s^{-1}).

$$k_{ex} = Z \exp(-\lambda/4RT) \qquad (23)$$

Assuming that the λ value for the electron-transfer disproportionation of $Me_2An^{\bullet+}$ is the same as that for the electron exchange between $Me_2An^{\bullet+}$ and Me_2An, the k_1 value is estimated from the λ and ΔG^0_{et} values as 3.0×10^3 M^{-1} s^{-1}. This value agrees well with the k_1 value (2.4×10^3 M^{-1} s^{-1}) in Table 1. Such an agreement between the k_1 value and the calculated value of the electron-transfer rate constant strongly supports that the observed second-order decay of $Me_2An^{\bullet+}$ is ascribed to electron-transfer disproportionation between $Me_2An^{\bullet+}$. The k_1 value of $Me_2An^{\bullet+}$ may be considered as the minimum value of the rate constant of electron-transfer disproportionation of anthracene radical cations, since the much stronger interaction of other anthracene dications with H_2O causes the negative shift in the E^0_{ox} value, resulting in the much larger k_1 values. The observed reactivity order of anthracene radical cations (An > EtAn > $PhCH_2An$ > Me_2An) may be determined by the thermodynamic stability of the complex formed between corresponding dication and H_2O. Thus, introduction of substituents at 9- and 10-positions of anthracene decreases the reactivity of electron-transfer disproportionation of the radical cation which is the rate-determining step for the multielectron oxidation of anthracenes.

Acknowledgment. We are grateful to Dr. M. Fujita for his valuable contribution in the early stage of the present work. This work was partially supported by a Grant-in-Aid for Scientific Research Priority Area (10149230 and 1025220) from the Ministry of Education, Science, Culture and Sports, Japan.

References and Notes

(1) (a) Parker, V. D. *Acc. Chem. Res.* **1984**, *17*, 243. (b) Hammerich, O.; Parker, V. D. *Adv. Phys. Org. Chem.* **1984**, *20*, 55.

(2) Bard, A. J.; Ledwith, A.; Shine, H. J. *Adv. Phys. Org. Chem.* **1976**, *12*, 115.

(3) (a) Bordwell, F. G. *Acc. Chem. Res.* **1988**, *21*, 456. (b) Bordwell, F. G.; Bausch, M. J. *J. Am. Chem. Soc.* **1986**, *108*, 2473. (c) Bordwell, F. G.; Cheng, J.-P.; Bausch, M. J. *J. Am. Chem. Soc.* **1988**, *110*, 2867. (d) Bordwell, F. G.; Cheng, J.-P. *J. Am. Chem. Soc.* **1989**, *111*, 1792. (e) Zhang, X.; Bordwell, F. G. *J. Org. Chem.* **1992**, *57*, 4163. (f) Zhang, X.-M.; Bordwell, F. G.; Bares, J. E.; Cheng, J.-P.; Petrie, B. C. *J. Org. Chem.* **1993**, *58*, 3051.

(4) (a) Nicholas, A. M. P.; Arnold, D. R. *Can. J. Chem.* **1982**, *60*, 2165. (b) Nicholas, A. M. P.; Arnold, D. R. *Can. J. Chem.* **1984**, *62*, 1850. (c) Nihcolas, A. M. P.; Arnold, D. R. *Can. J. Chem.* **1984**, *62*, 1860.

(5) (a) Fukuzumi, S.; Tokuda, Y.; Kitano, T.; Okamoto, T.; Otera, J. *J. Am. Chem. Soc.* **1993**, *115*, 8960. (b) Fukuzumi, S.; Koumitsu, S.; Hironaka, K.; Tanaka, T. *J. Am. Chem. Soc.* **1987**, *109*, 305.

(6) (a) Baciocchi, E.; Bietti, M.; Steenken, S. *J. Am. Chem. Soc.* **1997**, *119*, 4078. (b) Baciocchi, E.; Delgiacco, T.; Elisei, F. *J. Am. Chem. Soc.* **1993**, *115*, 12290. (c) Baciocchi, E.; Cort, A. D.; Eberson, L.; Mandolini, L.; Rol, C. *J. Org. Chem.* **1986**, *51*, 4544. (d) Baciocchi, E.; D'Acunzo, F.; Galli, C.; Lanzalunga, O. *J. Chem. Soc., Perkin Trans. 2* **1996**, 133. (d) Fujita, M.; Ishida, A.; Takamuku, S.; Fukuzumi, S. *J. Am. Chem. Soc.* **1996**, *118*, 8566.

(7) (a) Schlesener, C. J.; Amatore, C.; Kochi, J. K. *J. Am. Chem. Soc.* **1984**, *106*, 3567. (b) Schlesener, C. J.; Amatore, C.; Kochi, J. K. *J. Am. Chem. Soc.* **1984**, *106*, 7472.

(8) (a) Albini, A.; Sulpizio, A. In *Photoinduced Electron Transfer*; Fox, M. A., Chanon, M., Eds.; Elsevier: Amsterdam, 1988; Part C, p 88. (b) Albini, A.; Fasani, E.; Mella, M. *Topp. Curr. Chem.* **1993**, *168*, 143.

(9) (a) Parker, V. D.; Chao, E. T.; Zheng, G. *J. Am. Chem. Soc.* **1997**, *119*, 11390. (b) Reitstöen, B.; Norrsell, F.; Parker, V. D. *J. Am. Chem. Soc.* **1989**, *111*, 8463. (c) Parker, V. D.; Chao, Y. T.; Reitstöen, B. *J. Am. Chem. Soc.* **1991**, *113*, 2336. (d) Reitstöen, B.; Parker, V. D. *J. Am. Chem. Soc.* **1991**, *113*, 6954. (e) Reitstöen, B.; Parker, V. D. *J. Am. Chem. Soc.* **1990**, *112*, 4968. (f) Reitstöen, B.; Parker, V. D. *Acta Chem. Scand.* **1992**, *46*, 464.

(10) (a) Tolbert, L. M.; Khanna, R. K.; Popp, A. E.; Gelbaum, L.; Bottomley, L. A. *J. Am. Chem. Soc.* **1990**, *112*, 2373. (b) Sirimanne, S. R.; Li, Z. Z.; VanderVeer, D. R.; Tolbert, L. M. *J. Am. Chem. Soc.* **1991**, *113*, 1766. (c) Tolbert, L. M.; Li, Z. Z.; Sirimanne, S. R.; VanDerveer, D. G. *J. Org. Chem.* **1997**, *62*, 3927.

(11) (a) Tanko, J. M.; Wang, Y. *Chem. Commun.* **1997**, 2387. (b) Wang, Y.; Tanko, J. M. *J. Am. Chem. Soc.* **1997**, *119*, 8201.

(12) Eberson, L.; Blum, Z.; Helgée, B.; Nyberg, K. *Tetrahedron* **1978**, *34*, 731.

(13) Pross, A. *J. Am. Chem. Soc.* **1986**, *108*, 3537.

(14) (a) Parker, V. D.; Tilset, M. *J. Am. Chem. Soc.* **1987**, *109*, 2521. (b) Parker, V. D.; Tilset, M. *J. Am. Chem. Soc.* **1988**, *110*, 1649.

(15) (a) Shaik, S. S.; Pross, A. *J. Am. Chem. Soc.* **1989**, *111*, 4306. (b) Shaik, S.; Reddy, A. C.; Ioffe, A.; Dinnocenzo, J. P.; Danovich, D.; Cho, J. K. *J. Am. Chem. Soc.* **1995**, *117*, 3205.

(16) (a) Workentin, M. S.; Parker, V. D.; Morkin, T. L.; Wayner, D. D. M. *J. Phys. Chem. A* **1998**, *102*, 6503. (b) Workentin, M. S.; Schepp, N. P.; Johnston, L. J.; Wayner, D. D. M. *J. Am. Chem. Soc.* **1994**, *116*, 1141. (c) Workentin, M. S.; Johnston, L. J.; Wayner, D. D. M.; Parker, V. D. *J. Am. Chem. Soc.* **1994**, *116*, 8279.

(17) (a) Johnston, L. J.; Schepp, N. P. *J. Am. Chem. Soc.* **1993**, *115*, 6564. (b) Schepp, N. P.; Johnston, L. J. *J. Am. Chem. Soc.* **1994**, *116*, 6895. (c) Schepp, N. P.; Johnston, L. J. *J. Am. Chem. Soc.* **1994**, *116*, 10330.

(18) (a) Dockery, K. P.; Dinnocenzo, J. P.; Farid, S.; Goodman, J. L.; Gould, I. R.; Todd, W. P.; *J. Am. Chem. Soc.* **1997**, *119*, 1876. (b) Dinnocenzo, J. P.; Zuilhof, H.; Lieberman, D. R.; Simpson, T. R.; McKechney, M. W. *J. Am. Chem. Soc.* **1997**, *119*, 994. (c) Dinnocenzo, J. P.; Todd, W. P.; Simpson, T. R.; Gould, I. R. *J. Am. Chem. Soc.* **1990**, *112*, 2462. (d) Dinnocenzo, J. P.; Farid, S.; Goodman, J. L.; Gould, I. R.; Todd, W. P.; Mattes, S. L. *J. Am. Chem. Soc.* **1989**, *111*, 8973.

(19) (a) Brede, O.; David, F.; Steenken, S. *J. Chem. Soc., Perkin Trans. 2* **1995**, 23. (b) Koike, K.; Thomas, J. K. *J. Chem. Soc., Faraday Trans.* **1992**, *88*, 195.

(20) (a) Baciocchi, E.; Bietti, M.; Putignani, L.; Steenken, S. *J. Am. Chem. Soc.* **1996**, *118*, 5952. (b) Baciocchi, E.; Bietti, M.; Lanzalunga, O.: Steenken, S. *J. Am. Chem. Soc.* **1998**, *120*, 11516. (b) Steenken, S.; McClelland, R. A. *J. Am. Chem. Soc.* **1989**, *111*, 4967.

(21) (a) Bockman, T. M.; Hubig, S. M.; Kochi, J. K. *J. Am. Chem. Soc.* **1998**, *120*, 2826. (b) Hubig, S. M.; Bockman, T. M.; Kochi, J. K. *J. Am. Chem. Soc.* **1997**, *119*, 2926. (c) Hubig, S. M.; Bockman, T. M.; Kochi, J. K. *J. Am. Chem. Soc.* **1996**, *118*, 3842.

(22) (a) Majeski, E. J.; Stuart, J. D.; Ohnesorge, E. *J. Am. Chem. Soc.* **1968**, *90*, 633. (b) Parker, V. D. *Acta Chem. Scand.* **1970**, *24*, 2757.

(23) Evans, J. F.; Blount, H. N. *J. Phys. Chem.* **1979**, *83*, 1970.

(24) A preliminary report for the four-electron oxidation of 9-alkylanthracene with $Fe(ClO_4)_3 \cdot 9H_2O$ has appeared. Fujita, M.; Fukuzumi, S. *Chem. Lett.* **1993**, 1911.

(25) DeSimone, R. E.; Drago, R. S. *J. Am. Chem. Soc.* **1970**, *92*, 2343.

(26) Mauzerall, D.; Westheimer, F. H. *J. Am. Chem. Soc.* **1955**, *77*, 2261.

(27) Wong, C. L.; Kochi, J. K. *J. Am. Chem. Soc.* **1979**, *101*, 5593.

(28) Perrin, D. D.; Armarego, W. L. F.; Perrin, D. R. *Purification of Laboratory Chemicals*; Pergamon Press: Elmsford, 1966.

(29) Fukuzumi, S.; Kondo, Y.; Tanaka, T. *Chem. Lett.* **1983**, 485.

(30) Mann, C. K.; Barnes, K. K. *Electrochemical Reactions in Nonaqueous Systems*; Marcel Dekker: New York, 1990.

(31) Fukuzumi, S.; Nakanishi, I.; Tanaka, K.; Suenobu, T.; Tabard, A.; Guilard, R.; Van Caemelbecke, E.; Kadish, K. M. *J. Am. Chem. Soc.* **1999**, *2*, 785.

(32) The absorption spectrum of $RAn^{\bullet+}$ in Figure 1 is essentially the same as that of anthracene radical cation generated by the electrochemical oxidation, photoinduced electron transfer, and γ-irradiation. (a) Masnovi, J. M.; Kochi, J. K.; Hilinski, E. F.; Rentzepis, P. M. *J. Am. Chem. Soc.* **1986**, *108*, 1126. (b) Rodgers, M. A. *Trans. Faraday Soc.* **1971**, *67*, 1029. (c) Shida, T.; Iwata, S. *J. Am. Chem. Soc.* **1973**, *95*, 3473.

(33) The appearance of absorbance at 720 nm due to $An^{\bullet+}$ and the concomitant increase in absorbance at 450 nm due to $[Ru(bpy)_3]^{2+}$ were too fast to be followed by the stopped-flow technique.

(34) Streitwieser, A., Jr.; Jagow, R. H.; Fahey, R. C.; Suzuki, S. *J. Am. Chem. Soc.* **1958**, *80*, 2326.

(35) Kubota, T.; Kano, K.; Uno, B.; Konse, T. *Bull. Chem. Soc. Jpn.* **1987**, *60*, 3865.

(36) Fukuzumi, S.; Okamoto, T. *J. Am. Chem. Soc.* **1993**, *115*, 11600.

(37) Fukuzumi, S. *Bull. Chem. Soc. Jpn.* **1997**, *70*, 1.

(38) Fukuzumi, S.; Itoh, S. In *Advances in Photochemistry*; Neckers, D. C., Volman, D. H., Bünau, G., Eds.; Wiley: New York, 1999; Vol. 25, Chapter 3.

(39) (a) Marcus, R. A. *Annu. Rev. Phys. Chem.* **1964**, *15*, 155. (b) Marcus, R. A. *Angew. Chem., Int. Ed. Engl.* **1993**, *32*, 1111. (c) Eberson, L. *Adv. Phys. Org. Chem.* **1982**, *18*, 79.

(40) The hyperfine coupling constants for $Me_2An^{\bullet+}$ in Figure 11 (inset) agree with the reported values; see: Buchanan, A. C., III; Livingston, R.; Dworkin, A. S.; Smith, G. P. *J. Phys. Chem.* **1980**, *84*, 423.

(41) (a) Ward, R. L.; Weissman, S. I. *J. Am. Chem. Soc.* **1957**, *79*, 2086. (b) Chang, R. *J. Chem. Educ.* **1970**, *47*, 563. (c) Watts, M. T.; Lu, M. L.; Chen, R. C.; Eastman, M. P. *J. Phys. Chem.* **1973**, *77*, 2959. (d) Cheng, K. S.; Hirota, N. In *Investigation of Rates and Mechanisms of Reactions*; Hammes, G. G., Ed.; Wiley-Interscience: New York, 1974; Vol. VI, p 565. (e) Nakanishi, I.; Itoh, S.; Suenobu, T.; Fukuzumi, S. *Chem. Commun.* **1997**, 1927.